A Linear Active Disturbance Rejection Controller-Based Sensorless Control Scheme for PMSM Drives

Lizhi Qu, Liyan Qu, and Wei Qiao
Power and Energy Systems Laboratory
Department of Electrical and Computer Engineering
University of Nebraska−Lincoln
Lincoln, NE 68588-0511 USA
lizhi.qu@huskers.unl.edu; lqu2@unl.edu; wqiao3@unl.edu

***Abstract*—Sliding-mode observer (SMO)-based rotor position sensorless field-oriented control (FOC) methods have been widely employed for permanent-magnet synchronous motor (PMSM) drives used in electric vehicles. However, these methods have two main problems: phase delay and speed chattering. To cope with these two issues, a linear active disturbance rejection controller (LADRC)-based sensorless FOC scheme is proposed in this paper. The LADRC consists of a linear extended state observer (LESO) and a proportional current controller. The LESO is designed to estimate the back electromotive force (EMF) of the PMSM, which is treated as the external disturbance, without using any low-pass filter or switching function. Then, the rotor position and speed are obtained from the estimated back EMF without any phase delay or speed chattering problem. The estimated disturbance is used as a feedforward compensation term for the input of the plant. The plant combined with the LESO is equivalent to a zero-pole first-order system with a unity gain, which is controlled by a simple proportional current controller to generate the desired voltage vector for the pulse-width modulation (PWM) control of the PMSM inverter. The proposed LADRC-based sensorless FOC scheme is validated by both simulation and experimental results for a 275-W salient-pole PMSM drive in which the PMSM is similar to the traction motor used in Toyota Prius hybrid electric vehicles at a reduced scale.**

Keywords—Field oriented control (FOC), linear active disturbance rejection control (LADRC), linear extended state observer (LESO), permanent-magnet synchronous motor (PMSM), rotor position estimation, sensorless control.

I. INTRODUCTION

Permanent-magnet synchronous motors (PMSMs) have been widely employed in industrial applications owing to their high reliability, high efficiency, and high power density [1], [2]. To achieve high-performance control for PSMSs, electromechanical sensors, such as hall-effect sensors, optical encoders, and resolvers are commonly used. However, the use of these sensors not only increases the cost but also reduces the reliability of the PMSM drive systems [3]. Therefore, sensorless FOC of PMSM drives has been widely researched in the last few decades.

The sensorless FOC methods for salient-pole PMSMs can be generally classified into two categories: the high-frequency (HF) signal injection methods and the back electromotive force (EMF) estimation methods. For zero- and low-speed operations, the HF signal injection methods were well founded and exhibited satisfying performance [4], [5]. However, their capability of estimating the rotor position deteriorates dramatically in medium- to high- speed operations due to the limited control bandwidth.

The EMF estimation methods, by contrast, perform well in medium- and high-speed operations by observing the back EMF [6], [7]. The main technologies for the EMF observation include the direct calculation [8], the reduced-order extended Kalman filter (EKF) [9], and the sliding-mode observer (SMO) [7]. The direct calculation method is simple but is susceptible to machine parameter variations and sampling noise. Compared to the direct calculation method, the sampling noise can be eliminated and more accurate rotor position and speed estimation results can be obtained by using the reduced-order EKF method. However, the computational burden of the EKF method is heavier. Due to its simple algorithm and strong robustness to machine parameter variations, the SMO method has attracted more and more attention, especially in the applications of traction motor drives for hybrid electric vehicles. The defects of the SMO method are the speed chatting and phase delay problems. Plenty of work has been done to solve these two problems, such as using the sigmoid function instead of the sign function [10] and phase compensation [11]. However, the problems have not been completely solved. To solve the two problems completely, a disturbance observer [12] was proposed to estimate the back EMF. However, it is hard to design the gains of the disturbance observer due to the variations of the machine parameters used in the observer.

Recently, a method called active disturbance rejection control (ADRC) has been applied in motor drive systems [13], [14] because its design process does not rely on an accurate mathematical model of the system and it has a strong disturbance rejection capability. A robust control method that employed three first-order ADRCs was proposed for the speed control of an induction motor drive, which removed the need for the rotor flux estimation and reduced the computation burden [13]. In [14], an ADRC was combined with a model

This work was supported in part by the Nebraska Public Power District through the Nebraska Center for Energy Sciences Research and a University of Nebraska Collaboration Initiative Seed Grant.

predictive control for the speed loop of a PMSM drive system to enhance the system robustness to disturbances, including machine parameter variations and external load changes. However, little work has been reported on the application of the ADRC for position sensorless control of PMSM drives.

This paper proposes a novel linear ADRC (LADRC)-based rotor position sensorless FOC scheme for PMSM drives in an estimated synchronously rotating reference frame. The LADRC consists of a linear extended state observer (LESO) and a proportional current controller. The LESO is designed to estimate the back EMF, which is treated as an external disturbance, without using any low-pass filter or switching function. Then, the rotor position and speed are obtained from the estimated back EMF by using a tracking controller without any phase delay or speed chattering problem. The estimated disturbance, i.e., back EMF, is also used to compensate the input of the plant. In this way, the plant combined with the LESO is equivalent to a zero-pole first-order system, which can be controlled by a simple proportional current controller to generate the desired voltage vector for the PWM control of the PMSM inverter. The effectiveness of the LADRC-based sensorless FOC scheme is evaluated by both simulation and experimental results for a 275-W salient-pole PMSM drive.

II. Proposed LADRC-Based Rotor Position Sensorless FOC Scheme for PMSM Drives

A. Problem of the SMO-based Sensorless FOC for a PMSM

For a salient-pole PMSM, a back EMF-based model is commonly used, which can be written in a stationary $\alpha\beta$ reference frame according to [3] as follows:

$$\begin{bmatrix} v_{s\alpha} \\ v_{s\beta} \end{bmatrix} = \begin{bmatrix} R_s + pL_d & \omega_{re}(L_d - L_q) \\ \omega_{re}(L_q - L_d) & R_s + pL_d \end{bmatrix} \begin{bmatrix} i_{s\alpha} \\ i_{s\beta} \end{bmatrix} + \eta \begin{bmatrix} -\sin\theta_{re} \\ \cos\theta_{re} \end{bmatrix} \quad (1)$$

where $v_{s\alpha}$ and $v_{s\beta}$ are the α- and β-axis stator voltages, respectively; $i_{s\alpha}$ and $i_{s\beta}$ are the α- and β-axis stator currents, respectively; R_s is the stator armature resistance; L_d and L_q are the d- and q-axis inductances, respectively; ω_{re} is the rotor electrical angular speed; $p = d/dt$ is the time derivative operator; θ_{re} is the rotor position angle; and η is the magnitude of the back EMF, and can be written as:

$$\eta = (L_d - L_q)(\omega_{re} i_{sd} - p i_{sq}) + \omega_{re}\psi_m \quad (2)$$

where i_{sd} and i_{sq} are the d- and q-axis stator currents, respectively; and ψ_m is the rotor magnet flux linkage.

The last term on the right-hand side of (1) contains the information of the rotor position, and is called the back EMF. If the back EMF can be estimated by an observer, then the rotor position can be extracted by using an inverse tangent method or an angle tracking observer.

Among various types of observers, the SMO is a promising candidate for the back EMF estimation due to its simple algorithm and high robustness to the disturbance. The mathematical formulation of the SMO is expressed as:

$$\begin{cases} p\hat{i}_{s\alpha} = \dfrac{v_{s\alpha}}{L_d} - \dfrac{R_s}{L_d}\hat{i}_{s\alpha} + \hat{\omega}_{re}\dfrac{L_q - L_d}{L_d} i_{s\beta} + lZ_\alpha \\ p\hat{i}_{s\beta} = \dfrac{v_{s\beta}}{L_d} - \dfrac{R_s}{L_d}\hat{i}_{s\beta} + \hat{\omega}_{re}\dfrac{L_d - L_q}{L_d} i_{s\alpha} - lZ_\beta \end{cases} \quad (3)$$

where l is the observer gain; Z_α and Z_β are the α- and β-axis outputs of the sign functions, respectively; and $\hat{\omega}_{re}$ is the estimated rotor electrical angular speed. In practice, two low-pass filters are used after the outputs of the two sign functions to obtain the back EMF. Then, the rotor position can be obtained from the estimated back EMF by using a phase-locked loop (PPL). Fig. 1 shows the block diagram of the conventional SMO-based rotor position estimation method for the salient-pole PMSM. The low-pass filters need to be designed properly to mitigate the oscillating position error due to the unwanted noise caused by the sign function.

Due to the use of the low-pass filters, there is a phase delay in the estimated back EMF. Moreover, there is a speed chattering problem in the estimated back EMF due to the use of the discrete sign functions. These two problems usually make the system performance unsatisfactory. To solve the problems of the SMO-based rotor position estimation method, this paper proposes a LESO-based rotor position estimation method, as described in the next subsection.

B. Proposed LADRC-Based Sensorless FOC for a PMSM

A back EMF-based model for a salient-pole PMSM can be written in the synchronously rotating dq reference frame as follows:

$$\begin{bmatrix} v_{sd} \\ v_{sq} \end{bmatrix} = \begin{bmatrix} R_s + pL_d & -\omega_{re}\cdot L_q \\ \omega_{re}\cdot L_q & R_s + pL_d \end{bmatrix} \begin{bmatrix} i_{sd} \\ i_{sq} \end{bmatrix} + \begin{bmatrix} 0 \\ \eta \end{bmatrix} \quad (4)$$

where v_{sd} and v_{sq} are the d- and q-axis stator voltages, respectively.

However, in a sensorless drive system, such a dq model cannot be utilized since the rotor position θ_{re} is not measured. To solve this problem, an estimated synchronously rotating $\gamma\delta$ reference frame instead of the actual synchronously rotating dq reference frame is used, as shown in Fig. 2. Then, a rotor position estimation error $\Delta\theta_{re}$ is defined as:

$$\Delta\theta_{re} = \hat{\theta}_{re} - \theta_{re} \quad (5)$$

where $\hat{\theta}_{re}$ is the rotor position estimated in the $\gamma\delta$ reference frame.

By transforming (4) into the $\gamma\delta$ reference frame, the back

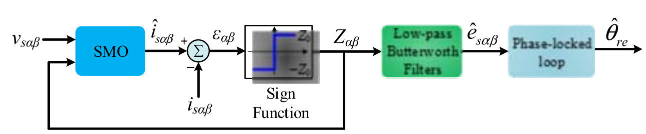

Fig. 1. Block diagram of the SMO-based rotor position estimation for the salient-pole PMSM.

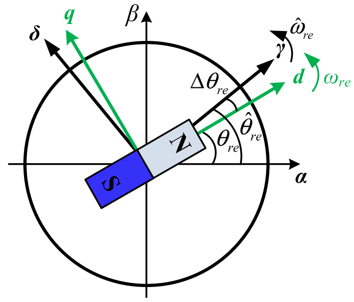

Fig. 2. The estimated $\gamma\delta$ reference frame and the dq reference frame.

EMF-based PMSM model can be expressed as:

$$\begin{bmatrix} v_{s\gamma} \\ v_{s\delta} \end{bmatrix} = \begin{bmatrix} R_s + pL_d & -\hat{\omega}_{re} \cdot L_q \\ \hat{\omega}_{re} \cdot L_q & R_s + pL_d \end{bmatrix} \begin{bmatrix} i_{s\gamma} \\ i_{s\delta} \end{bmatrix} + \begin{bmatrix} e_{s\gamma} \\ e_{s\delta} \end{bmatrix} \tag{6}$$

where $v_{s\gamma}$ and $v_{s\delta}$ are the γ- and δ-axis stator voltages, respectively; $i_{s\gamma}$ and $i_{s\delta}$ are the γ- and δ-axis stator currents, respectively; and $e_{s\gamma}$ and $e_{s\delta}$ are the γ- and δ-axis back EMF components, respectively, which can be expressed as:

$$\begin{bmatrix} e_{s\gamma} \\ e_{s\delta} \end{bmatrix} = \eta \begin{bmatrix} -\sin \Delta\theta_{re} \\ \cos \Delta\theta_{re} \end{bmatrix} + (\hat{\omega}_{re} - \omega_{re}) \cdot L_q \begin{bmatrix} -i_{s\gamma} \\ i_{s\delta} \end{bmatrix} \tag{7}$$

If $\hat{\omega}_{re} \approx \omega_{re}$, $\Delta\theta_{re}$ can be calculated as $\Delta\theta_{re} = -\tan^{-1}(e_{s\gamma} / e_{s\delta})$ according to (7). Moreover, if $e_{s\gamma} / L_d$ and $e_{s\delta} / L_d$ are treated as the γ- and δ-axis unknown external disturbances f_{e_γ} and f_{e_δ}, respectively, which contain the information of the γ- and δ-axis back EMF components and rotor position estimation error, the current model of the salient-pole PMSM can be written as:

$$\begin{cases} pi_{s\gamma} = v_{s\gamma} / L_d + f_\gamma - f_{e_\gamma} \\ pi_{s\delta} = v_{s\delta} / L_d + f_\delta - f_{e_\delta} \end{cases} \tag{8}$$

where $f_\gamma = \hat{\omega}_{re} \cdot L_q \cdot i_{s\delta} / L_d - R_s \cdot i_{s\gamma} / L_d$ and $f_\delta = -\hat{\omega}_{re} \cdot L_q \cdot i_{s\gamma} / L_d - R_s \cdot i_{s\delta} / L_d$, which represent the γ- and δ-axis known model information, respectively.

Then, a LESO-based external disturbance observer can be designed as:

$$\begin{cases} p\hat{i}_{sx} = v_{sx} / L_d + f_x - \hat{f}_{e_x} - L_{x1} \cdot \varepsilon_x \\ p\hat{f}_{e_x} = -L_{x2} \varepsilon_x \end{cases} \quad x = \gamma \text{ and } \delta \tag{9}$$

where $\hat{i}_{sx}$ is the estimated stator current; $\varepsilon_x = \hat{i}_{sx} - i_{sx}$ is the stator current estimation error; $\hat{f}_{e_x}$ is the estimated unknown external disturbance; and L_{x1} and L_{x2} are the gains of the LESO. The values of L_{x1} and L_{x2} can be determined according to the desired bandwidth of the LESO [15], which should be large enough to ensure that the dynamics of the LESO is sufficiently fast to track the variation of the disturbance. For example, the values of L_{x1} and L_{x2} can be simply determined such that the tracking error state equation of the LESO has the desired bandwidth.

Then, a tracking controller [16] can be designed to estimate the rotor position and speed by simply using a PLL to regulate the normalized value of the estimated γ-axis unknown external disturbance $\hat{f}_{e_\gamma}$, which contains the rotor position error information, to be zero, as shown in Fig. 3. The normalization of the back EMF components guarantees a constant linear dynamic response of the tracking controller regardless of the operating fundamental frequency.

According to the ADRC theory [17], the estimated disturbance is used as a feedforward compensation term for the input of the plant, as shown in Fig. 4. The combination of the plant and the LESO is equivalent to a zero-pole first-order system $1/s$ in the Laplace domain. Then, a simple proportional current controller k_{px} can be designed to generate the voltage output v_{sx0}, which is compensated by the disturbance estimated by the LESO to generate the voltage output v_{sx} of the LADRC, i.e., $v_{sx} = v_{sx0} - L_d(\hat{f}_{e_x} + f_x)$, for controlling the plant.

Compared to the conventional SMO-based method, there are two improvements in the proposed LESO-based rotor position estimation scheme. Firstly, by applying the estimated synchronously rotating reference frame instead of the stationary reference frame in the SMO-based method, the back EMF is transformed into DC components, which removes the need for the low-pass filter and, therefore, eliminates the phase delay in the estimated position. Secondly, due to the use of a continuous integrator $1/s$ in the LESO to estimate the back EMF components, the speed chattering problem caused

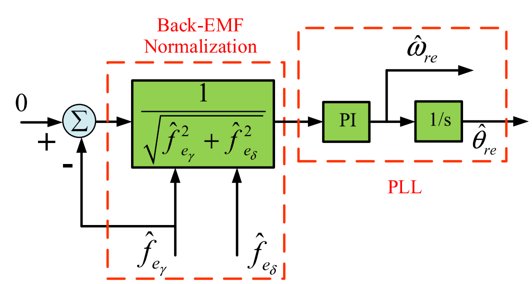

Fig. 3. Block diagram of the tracking controller for rotor position and speed estimation.

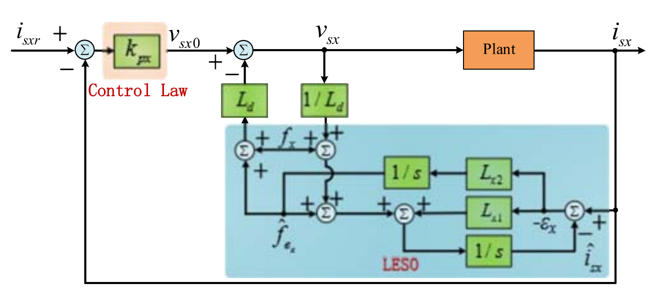

Fig. 4. Block diagram of the plant controlled by the LADRC scheme.

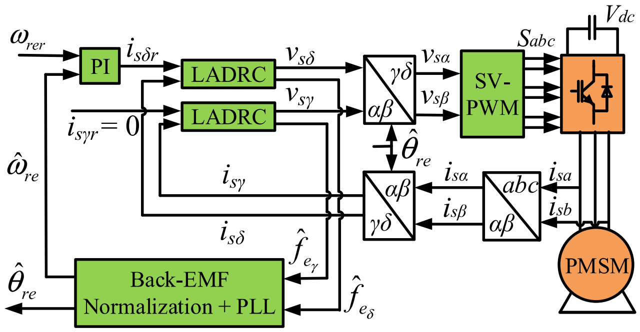

Fig. 5. Block diagram of the LADRC-based sensorless FOC scheme for a PMSM drive.

by the discrete sliding-mode function in the SMO is eliminated. Fig. 5 shows the block diagram of the overall LADRC-based rotor position sensorless FOC scheme for a PMSM drive, where the PMSM, inverter, SVPWM, and coordinate transformation blocks form the plant in Fig. 4.

III. Simulation Results

Simulation studies were carried out in MATLAB/Simulink to evaluate the proposed LADRC-based rotor position sensorless FOC scheme in comparison with the conventional SMO-based rotor position sensorless FOC scheme [18] for a 275-W salient-pole PMSM drive. The PMSM is similar to the traction motor used in Toyota Prius but has a reduced scale. The parameters of the PMSM are given as follows. The maximum speed is 3100 rpm; the rated load torque is 1.8 N·m; the stator resistance is R_s = 0.268 Ω; the d-axis stator inductance is L_d = 1.12 mH; the q-axis stator inductance is L_q = 1.51 mH; the rotor magnet flux linkage is ψ_m = 0.0191 V·s; the voltage constant is K_e = 13.5 mV/rpm; the number of pole pairs is n_p = 2; and the moment of inertia is J = 0.000007 kg·m^2. The DC bus voltage of the inverter is 41.75 V. The switching frequency of the inverter and the sampling frequency are both 10 kHz. The same PI controller is used for the speed loops of the two rotor position sensorless FOC schemes. In the SMO-based sensorless FOC scheme, the traditional PI controller is used in the current loop. The bandwidth of the speed-loop PI controller is selected as 200 Hz. The bandwidth of the current-loop PI controllers of the conventional SMO-based sensorless FOC system is chosen as 2000 Hz according to [19]. The parameters of the LADRC-based sensorless FOC system are designed as follows: the bandwidth of the LESO is designed as 2000 Hz as a tradeoff between current tracking performance and immunity to noise; and the parameter K_p of the current controller is set as 500 according to [15].

The position estimation performance of the two sensorless FOC schemes is compared for the salient-pole PMSM operating at 1500 rpm, where the command of the torque is 1.8 N·m. Assume that the d- and q-axis inductances used by the two schemes are mismeasured to be 150% of L_d and L_q from 0.05 s onwards. The rotor positions, rotor position estimation errors, and rotor speed estimation errors of the system using the two control schemes are compared in Fig. 6. The simulation results show that the rotor position and speed estimation errors of the proposed LADRC-based sensorless FOC scheme are 4.0 degree and 4.7 rpm, respectively, which are much smaller than 8.2 degree and 8.0 rpm, respectively, of the conventional SMO-based sensorless FOC scheme before the parameter mismatch occurs. After the parameter mismatch

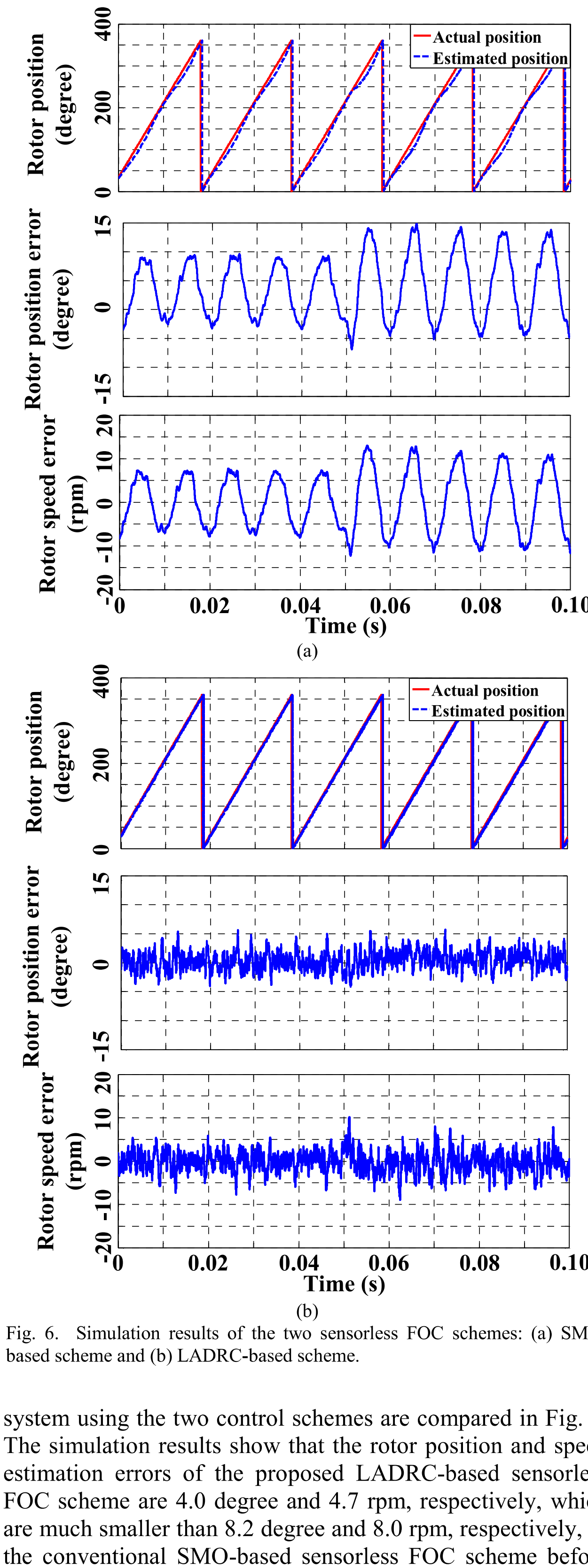

Fig. 6. Simulation results of the two sensorless FOC schemes: (a) SMO-based scheme and (b) LADRC-based scheme.

occurs, the rotor position and speed estimation errors increase from 7.2 degree to 9.8 degree and from 8.0 rpm to 10.8 rpm, respectively, when using the conventional SMO-based sensorless FOC scheme. However, with the help of the LESO for estimating and compensating the external disturbance in the LADRC-based sensorless FOC scheme, the rotor position and speed estimation performance is not affected by the parameter mismatch at all. Meanwhile, the phase delay and speed chattering problem in the SMO-based sensorless FOC scheme are resolved in the proposed method as well.

IV. Experimental Results

Experimental studies were carried out to further evaluate the proposed LADRC-based sensorless FOC scheme in comparison with the conventional SMO-based sensorless FOC scheme for the 275-W salient-pole PMSM drive used in the simulation studies. The control algorithms were implemented in a dSPACE 1104 real-time control system with a sampling period of 100 μs. The dead time was set as 1 μs. The block diagram and hardware setup of the experiment system are shown in Figs. 7 and 8, respectively. In the experimental studies, the parameters are set to be the same with those in the simulation studies. Experiments were performed on the system at the same operating condition evaluated in the simulation study in Section III, and the results are compared in Fig. 9. It can be seen that the experimental results agree with the simulation results. These results show that the LADRC-based sensorless FOC scheme has better rotor position and speed estimation performance than the conventional SMO-based sensorless FOC scheme by timely estimating and compensating the external disturbance. Moreover, the phase delay and speed chattering problem in the conventional SMO-based sensorless FOC scheme are resolved in the proposed LADRC-based sensorless FOC scheme as well.

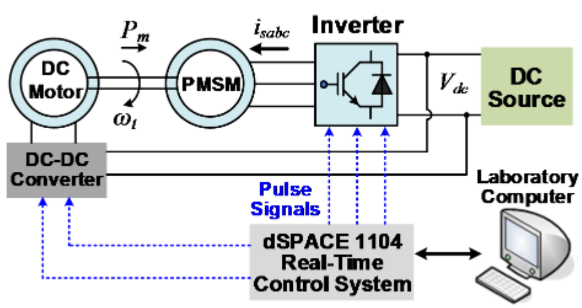

Fig. 7. Block diagram of the experiment system.

Fig. 8. Hardware setup of the experiment system.

V. Conclusion

A LADRC-based rotor position sensorless FOC scheme

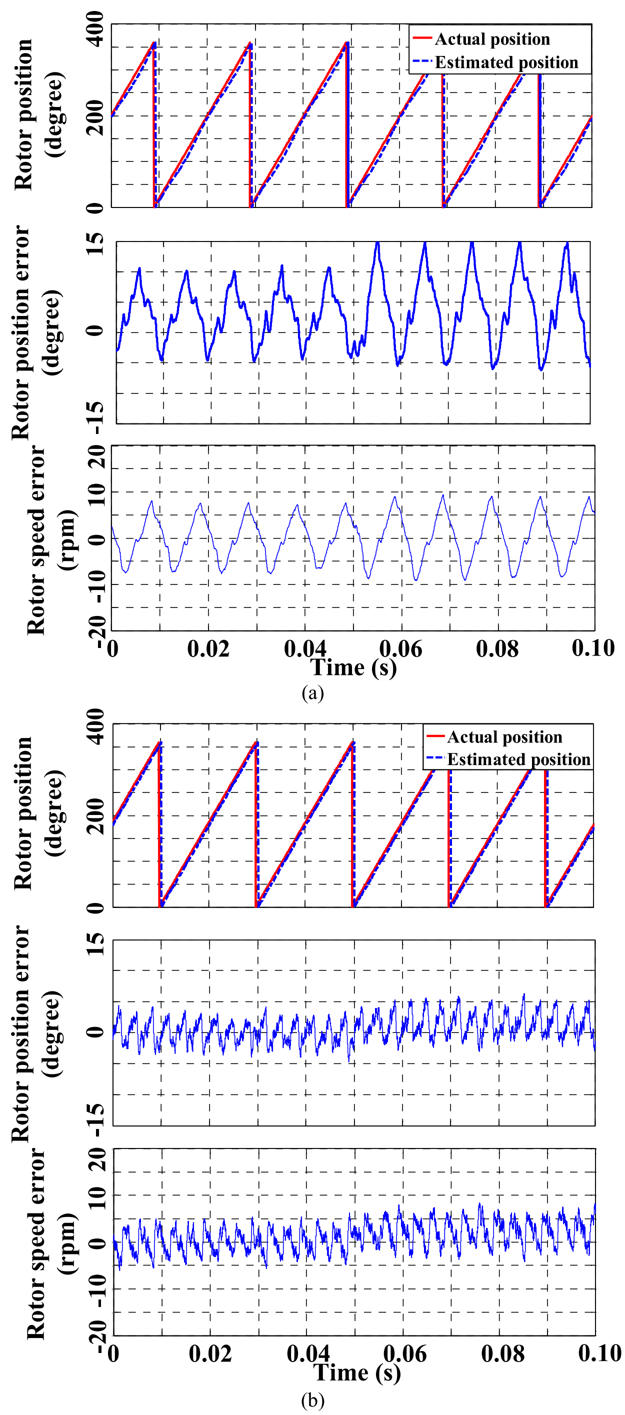

Fig. 9. Experimental results of the two sensorless FOC schemes: (a) SMO-based scheme and (b) LADRC-based scheme.

was proposed for PMSM drive systems in an estimated synchronously rotating reference frame. The proposed sensorless FOC resolved the phase delay and speed chattering problems in the conventional SMO-based sensorless FOC schemes. The performance of the proposed LADRC-based sensorless FOC scheme was validated by both simulation and experimental results for a 275-W salient-pole PMSM drive. The simulation and experimental results showed that the PMSM drive using the LADRC-based scheme was not affected by PMSM parameter mismatches at all and had better rotor position estimation performance than the conventional SMO-based sensorless FOC scheme.

REFERENCES

[1] N. Zhao, G. Wang, D. Xu, L. Zhu, G. Zhang, and J. Huo, "Inverter power control based on DC-Link voltage regulation for IPMSM drives without electrolytic capacitors," *IEEE Trans. Power Electron.*, vol. 33, no. 1, pp. 558-571, Jan. 2018.

[2] G. Wang, L. Qu, H. Zhan, J. Xu, L. Ding, G. Zhang, and D. Xu, "Self-commissioning of permanent magnet synchronous machine drives at standstill considering inverter nonlinearities," *IEEE Trans. Power Electron.*, vol. 29, no. 12, pp. 6615-6627, Dec. 2014.

[3] Y. Zhao, C. Wei, Z. Zhang, and W. Qiao, "A review on position/speed sensorless control for permanent-magnet synchronous machine-based wind energy conversion systems," *IEEE J. Emerging Sel. Topics Power Electron.,* vol. 1, no. 4, pp. 203-216, Dec. 2013.

[4] M. J. Corley and R. D. Lorenz, "Rotor position and velocity estimation for a salient-pole permanent magnet synchronous machine at standstill and high speeds," *IEEE Trans. Ind. Appl.*, vol. 34, no. 4, pp. 784-789, Jul./Aug. 1998.

[5] S. Kim, J. Im, E. Song, and R. Kim, "A new rotor position estimation method of IPMSM using all-pass filter on high-frequency rotating voltage signal injection," *IEEE Trans. Ind. Electron.*, vol. 63, no. 10, pp. 6499-6509, Oct. 2016.

[6] J. Liu, T. A. Nondahl, P. B. Schmidt, S. Royak, and M. Harbaugh, "Rotor position estimation for synchronous machines based on equivalent EMF," *IEEE Trans. Ind. Appl.*, vol. 47, no. 3, pp. 1310-1318, May/Jun. 2011.

[7] J. Kim, I. Jeong, K. Nam, J. Yang, and T. Hwang, "Sensorless control of PMSM in a high-speed region considering iron loss," *IEEE Trans. Ind. Electron.*, vol. 62, no. 10, pp. 6151-6159, Oct. 2015.

[8] D. Paulus, J. F. Stumper, and R. Kennel, "Sensorless control of synchronous machines based on direct speed and position estimation in polar stator-current coordinates," *IEEE Trans. Power Electron.*, vol. 28, no. 5, pp. 2503-2513, May 2013.

[9] N. K. Quang, N. T. Hieu, and Q. P. Ha, "FPGA-based sensorless PMSM speed control using reduced-order extended Kalman filters," *IEEE Trans. Ind. Electron.*, vol. 61, no. 12, pp. 6574-6582, Dec. 2014.

[10] H. Kim, J. Son, and J. Lee, "A high-speed sliding-mode observer for the sensorless speed control of a PMSM," *IEEE Trans. Ind. Electron.*, vol. 58, no. 9, pp. 4069-4077, Sept. 2011.

[11] X. Song, J. Fang, B. Han, and S. Zheng, "Adaptive compensation method for high-speed surface PMSM sensorless drives of EMF-based position estimation error," *IEEE Trans. Power Electron.*, vol. 31, no. 2, pp. 1438-1449, Feb. 2016.

[12] Z. Chen, M. Tomita, S. Doki, and S. Okuma, "An extended electromotive force model for sensorless control of interior permanentmagnet synchronous motors," *IEEE Trans. Ind. Electron.*, vol. 50, no. 2, pp. 288-295, Apr. 2003.

[13] J. Li, H. Ren, and Y. Zhong, "Robust speed control of induction motor drives using first-order auto-disturbance rejection controllers," *IEEE Trans. Ind. Appl.*, vol. 51, no. 1, pp. 712-720, Jan./Feb. 2015.

[14] G. Wang, Y. Wang, J. Xu, N. Zhao, and D. Xu, "Weight-transducerless rollback mitigation adopting enhanced MPC with extended state observer for direct-drive elevators," *IEEE Trans. Power Electron.*, vol. 31, no. 6, pp. 4440-4451, Jun. 2016.

[15] Z. Gao, "Scaling and bandwidth-parameterization based controller tuning," in *Proc. American Control Conference*, Jun. 2003, pp. 4989-4996.

[16] G. Zhang, G. Wang, D. Xu, and Y. Yu, "Discrete-time low-frequency-ratio synchronous-frame full-order observer for position sensorless IPMSM drives," *IEEE J. Emerg. Sel. Topics Power Electron.*, vol. 5, no. 2, pp. 870-879, Jun. 2017.

[17] J. Han, "From PID to active disturbance rejection control," *IEEE Trans. Ind. Electron.*, vol. 56, no. 3, pp. 900-906, Mar. 2009.

[18] Y. Zhao, W. Qiao, and L. Wu, "Improved rotor position and speed estimators for sensorless control of interior permanent-magnet synchronous machines," *IEEE J. of Emerg. Sel. Topics Power Electron.*, vol. 2, no. 3, pp. 627-639, Sept. 2014.

[19] K. J. Astrom and T. Hagglund, *Advanced PID Control*, ISA-Instrumentation, Systems, and Automation Society, 2006.